

Terahertz metamaterial absorber design and parametric analysis for Quad/-Penta and Hexa band applications

AMIT KUMAR VARSHNEY^{1,*}, N. SARAVANAKUMAR², P. SRIDHAR³

¹Dept. of ECE, Saveetha Engineering College, Chennai, Tamil Nadu, India

²Department of ECE, Dr. Mahalingam College of Engineering & Technology, Pollachi, Tamil Nadu, India

³Department of ECE, Sri Ramakrishna Engineering College, Coimbatore, Tamilnadu, India

In this paper, a polarization- and angle-insensitive terahertz (THz) metamaterial absorber (MMA) is designed and simulated for quad-, penta-, and hexa-band applications. Without using multiple layers or multiple resonators in a single unit cell, the proposed absorber contains only three layers. A dielectric substrate is placed in between the ground-plane and top patch resonator. The top simple patch planar structure consists of a square and an eclipse-shaped structure. From the parametric study, three designs are developed for quad-, penta-, and hexa-band operation with the maximum absorption rate. To analyze the physical structure of the MMA, parameter values with resonant frequency, electric field, magnetic field, and surface current distribution are simulated, and the results are presented. The polarization and angle-insensitive characteristics of the MMA are explained by varying the angle values from zero degrees to ninety degrees. Within the small frequency range (0.1–0.35) THz, the quad-, penta-, and hexa-bands are achieved without overlapping. This structure will be used for sensing, polarization imaging, and multiband applications.

(Received May 15, 2023; accepted November 24, 2023)

Keywords: Quad-/Penta and Hexa band, Polarization and incident angle insensitive, Parametric study

1. Introduction

Due to a number of unresolved electric and magnetic characteristics, with near-perfect absorption, ultra-thin dielectric layer thickness, and flexible expansion of the absorption bandwidth, MMAs, as a significant branch of metamaterial (MM) resonant devices, have involved significant research interest [1-3]. The thickness of MMA, mostly the thickness of their middle dielectric layer, is only an insufficient tenth or even one hundredth of the resonance wavelength, which stretches MMA the benefits of light weight and simple structure. This contrasts with the great and majority thickness of outdated absorbers, such as Salisbury screens and Jaumann absorbers [4]. It was measured that the first MMA occupied in the microwave area used a sandwich structure comprising of a lossy dielectric, a metallic cut wire, and an electric metallic split ring [5]. It is conceivable to realise almost whole absorption in this construction by concurrently suppressing transmission and reflection. Since then, numerous changed kinds of MMAs have been broadly presented, and their operating frequencies have regularly enlarged to contain all frequency ranges connected to technology slightly than just microwaves. For example, a MMA in the frequency range of 0.8-1.8 THz was verified employing an array of metallic rings set on a metallic bottom plane and separated by a dielectric spacer [6]. To realize near-unity absorption in the optical domain, a surface building created on patch antennas was planned [7]. To attain high absorption, mid-infrared reconfigurable MMAs with several surface structure plans were projected.

A square patch with a circular incision in the middle and four semi-circular cuts in the middle of each side kind of the surface structure of a MMA that works in the radio

band (30-300 MHz) [8]. In terms of medical imaging, bolometer, optical and microwave switch, refractive index (RI) sensor, solar cell, stealth technology, these proven MMAs are hopeful. But keep in mind that the mainstream of these MMAs only display single-band absorption, severely restrictive their imaginable for use. MMAs with frequent absorption peaks are projected and compulsory to growth the application options and possible of the absorption devices [9-11]. Double-band absorption, tri-band absorption, four-band absorption, etc. are some of the classifications given to the multiple-band MMAs created on the number of absorption peaks. To meet various application requirements, researchers are free to extent various sorts of multiple-band absorption devices [12-15].

As the number of absorption peaks rises, academics typically agree that more sophisticated metamaterial structure designs correspond to more absorption peaks. To produce dual-band absorption, for instance, metamaterial structures made of two distinct resonators of different sizes, such as synthetic insulator molecules and decorated graphene arrays, have been proposed. The prerequisites for achieving triple-band absorption are three sub-resonators with distinct sizes or geometries. It is possible to create four band absorption devices by joining increasingly sophisticated components [16-18].

This seems to become a never-ending cycle. We need to integrate or create extra sub resonators in the essential compartment of the absorption devices in order to produce many absorption peaks, particularly more absorption peaks. Unfortunately, the design approach for this particular vicious loop will result in or bring about numerous problems. First off, the presence of several sub-resonators in the fundamental cell invariably causes significant interactions between them, which lowers the

absorbance of the absorption devices. Also, the many sub-resonators in the fundamental cell will pose significant difficulties for the absorption devices total dimensions and engineering complexity. Thirdly, the absorption peaks cannot be greatly raised due to the quantity of sub resonators combined in the basic cell. Given these problems, it is preferable to minimise the quantity of resonators in order to develop multiple band absorption devices. The problem will be resolved more effectively if there are less resonators.

However, when many sub resonators are combined into a array structure, it frequently leads to large-scale unit dimensions that go against the current design trend of compactness and downsizing. The large and multiple resonator structure, which also raises gradually difficult as the number of absorption peaks rises, ultimately results in strong interactions between these sub-resonators, lowering or weakening the overall absorption strength of multiple band absorption devices. Accomplishing multiple band absorption with satisfactory presentation to switch a variation of applications is thus still a key topic in the study of MMs [19-21].

The terahertz metamaterial absorbers we suggest in this paper consist of a continuous metallic ground plane, a metallic surface structure, and a dielectric spacer. The top metallic structure consists of square shaped resonator. From that one horizontal and one vertical eclipse structure is etched and one horizontal and one vertical eclipse structure is added inside the etched eclipse structure. When we vary the inner eclipse x and y radius value, number of resonance bands and resonant frequency is also varied and this initial structure gives the quad band operation. It gives the Penta band operation when we change the inner eclipse y-radius value. Same structure gives the hexa band operation while deleting the total inner eclipse. These are all explained under different developing stages of MMA design. Without using different type of layers or multiple Resonators in a single unit cell, the proposed absorber contains only three layers, polyimide substrate is placed in between the ground

copper plane and top copper patch resonator. Parametric study is the important part to achieve a quad-/Penta and hexa bands in one single structure. The physical structure is analysed by electric field (E), magnetic field distribution (H) and surface current distribution. Polarization and angle insensitive characteristics curves are explained. This work is compared with previous bi/tri absorption functional works and it is shown in table 4 with references [22-30].

2. Structure and design

The quad-/penta- and hexa band operation is designed and simulated using the commercial CST Microwave Studio Software. Figure 1 depicts the MMA's perspective view. Dielectric substrate is positioned between the top and bottom copper planes in the simple three-layer structure. The substrate in use here is polyimide, which has a loss tangent ($\tan \delta$) of 0.0027 and a dielectric constant (ϵ_r) of 3.5. The metal employed in this situation is copper, which has a conductivity of $\sigma=5.8 \times 10^7$ S/m. Table 1 displays the design criteria for each of the three designs.

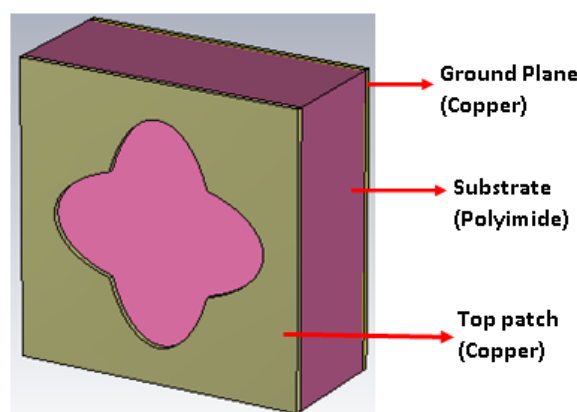


Fig. 1. Perspective view of the hexa band MMA (color online)

Table 1. Design Parameters of the proposed MMA.

Parameters	Values (mm)
Length and Width of the patch resonator	(0.45×0.45)
Y and X radius of the etched eclipse (R5×R6)	(0.34×0.18) Design-3- HEXA BAND
Y and X radius of the centre eclipse (R4×R3)	(0.01×0.12) Design-2- PENTA BAND
Y and X radius of the centre eclipse (R2×R1)	(0.11×0.12) Design-1- QUAD BAND
Substrate thickness	0.37
Bottom layer Thickness	0.018
Top Patch Thickness	0.018

2.1. Different developing stages of the MMA

Fig. 2 shows the different developing stages of the quad-/penta and hexa band MMA. Parametric study is an important part to get a three different operation in one single MMA structure. The design parameters which are used to design the quad-/penta and hexa operation is shown in Table 1. In all the three designs ground and

substrate layer length and width value is same. The ground and top copper layer thickness is 0.018 mm. The dielectric layer thickness is 0.37 mm.

In this work, the top patch design having square patch resonator, from that one horizontal and one vertical eclipse structure is etched and one horizontal and one vertical eclipse structure is added inside the etched eclipse structure. When we varying the inner eclipse Y radius

value, number of resonance bands and resonant frequency is also varied based on the parameter values this structure gives the quad-/penta and hexa bands. Fig. 2(a) shows the first structure which gives the quad band operation when the Y and X radius of the centre eclipse structure is (0.11×0.12) mm. If the Y and X radius of the centre

eclipse structure is (0.01×0.12) mm the structure gives the penta band operation which is shown in Fig. 2 (b). Fig. 3 is a simple planar patch structure which consists of square patch resonator and the eclipse shaped structure is etched from the square resonator. And this design gives the hexa band operation.

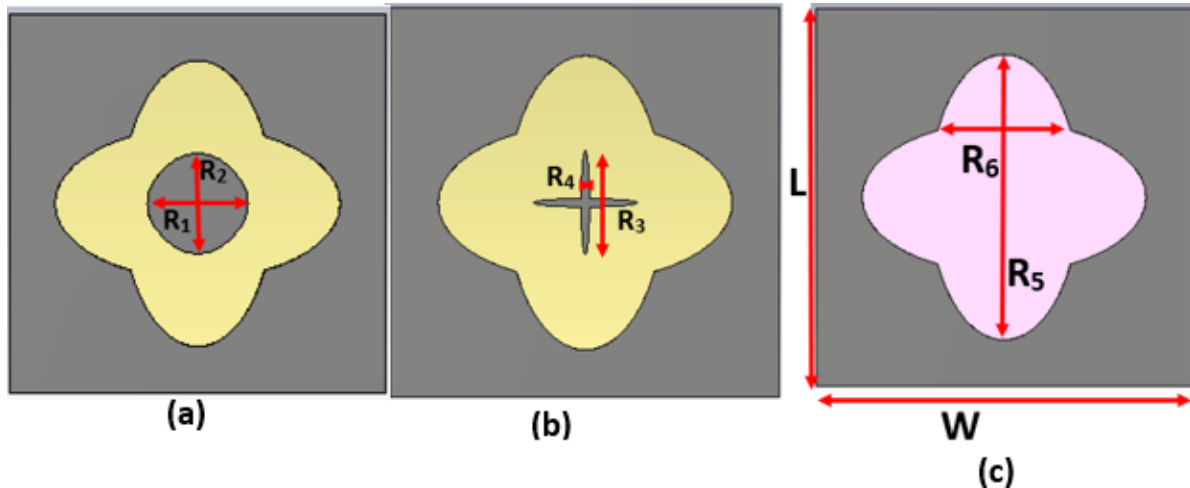


Fig. 2. Different developing stages of the quad-/penta and hexa band MMA (a) Quad band (b) Penta band (c) Hexa band, (Grey colour represents the copper, yellow and pink layer represents the polyimide substrate) (color online)

2.2. Boundary and Port conditions in MMA

For the simulations, a unit cell's x and y boundary conditions were periodic, and the z plane's boundary condition was an exact match for an open layer which is shown in Fig. 3. The absorption rate of the MMA is calculated by $Abs(\omega) = 1 - Ref(\omega) - Tra(\omega)$. Absorption, Reflection and Transmission is represented by Abs, Ref,

and Tra respectively. ω is the angular frequency. The transmission spectra demonstrate zero transmission due to the existence of a thick metallic ground metal layer that is bigger than its skin depth (δ) value. As a result, absorption is solely determined by the reflection component. Since the suggested form provides superior reflections in the necessary bands, absorption is enhanced.

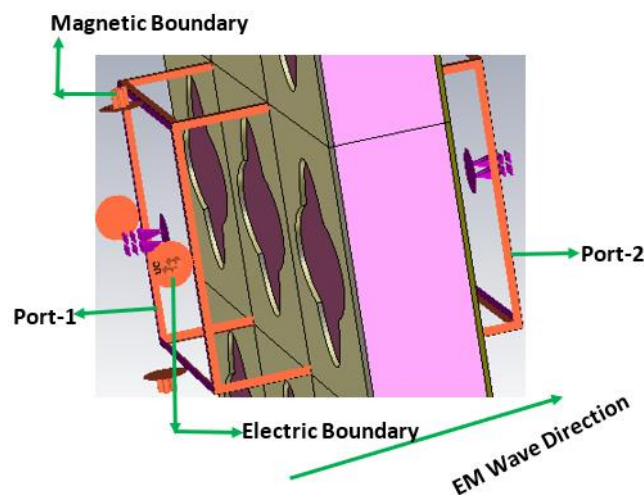


Fig. 3. Boundary condition and port places in MMA (color online)

3. Results and discussions

3.1. Resonant frequency and absorption rate of MMA

Fig. 4 shows the different developing stages of the MMA. From that, design 1 produces the quad band

operation and design 2 resonated at five different bands which is shown in Fig. 4 (a) and (b) respectively. Design 1 is resonated at four different bands at 0.143 THz, 0.170 THz, 0.220 THz and 0.276 THz with the absorption rate of 94.6 % ,99.6 % ,92 % and 85% respectively. And design 2 produces the five different bands at 0.145 THz, 0.172 THz, 0.224 THz, 0.283 THz and 0.310 THz with the

absorption rate of 92 %, 96.6 %, 99.7 %, 94.3 %, and 90 % respectively.

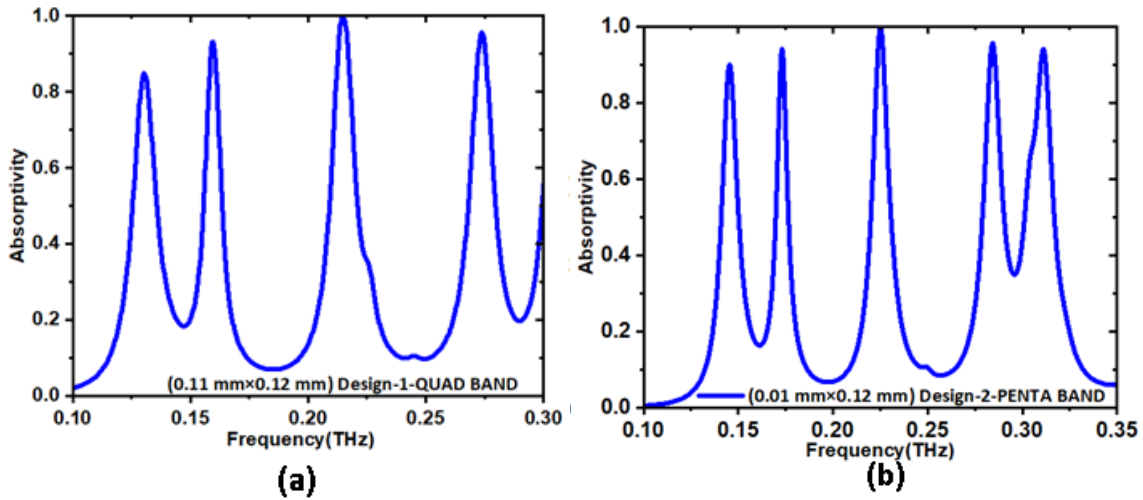


Fig. 4. Quad band and Penta band operation of an MMA (color online)

Table 2. Frequency and Absorption Rate of Quad-/Penta and Hexa band Absorber

Design	Number of Bands	Frequency (THz)	Absorptivity (%)
3	6	0.146, 0.174, 0.227, 0.288, 0.315, 0.328	92, 93, 99.9, 88.5, 97, 82
2	5	0.145, 0.172, 0.224, 0.283, 0.310	92, 96.6, 99.7, 94.3, 90
1	4	0.143, 0.170, 0.220, 0.276	94.6, 99.6, 92, 85

From the parametric analysis best number of bands is chosen based on the eclipse x and y radius value. Design 3 is a simple planar MMA absorber structure which presents the six-band operation. Fig. 5 (a) shows the hexa band operation characteristics curves for both transverse electric (TE) and transverse magnetic (TM) mode operation and 5 (b) shows the comparison curves for quad-/penta and hexa band operation. The six bands are occurred in 0.146 THz,

0.174 THz, 0.227 THz, 0.288 THz, 0.315 THz and 0.328 THz with the absorption rate of 92 %, 93 %, 99.9%, 88.5 %, 97 % and 82 % respectively. Table 2 shows the comparison table for quad-/penta and hexa band operation with respect to resonance frequency and absorption rate.

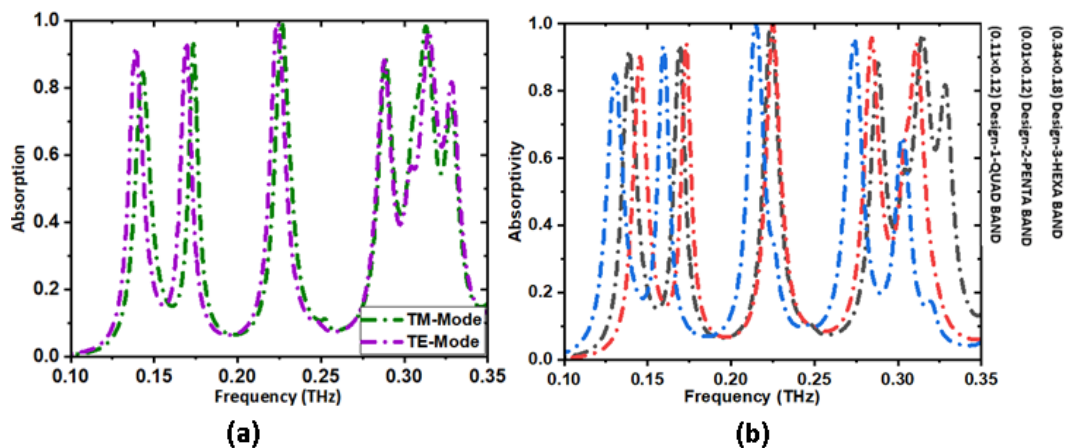


Fig. 5 (a). Hexa band operation of an MMA, (b) Comparison graph for quad-/penta and hexa band operation (color online)

3.2. Parametric study for Quad-/Penta band operation

Examining the parameters in MMA design from Fig. 2 (a) and (b), gives the chance to chose the best absorption

rate value which is shown in Fig. 6. In Fig. 6, ‘x’ radius value is fixed as 0.12 mm after some parametric examination and ‘y’ value is varied from 0.01 mm to 0.14 mm. When the ‘x’ radius value is 0.12 mm and ‘y’ radius value is 0.11 mm the structure gives the quad band

operation with high absorption rate compare to other values. When the ‘x’ radius value is 0.12 mm and ‘y’ radius value is 0.01 mm the structure gives the penta band

operation with high absorption rate compare to other values. So, the best absorption rate is fixed at different frequency values which is shown in Fig. 6.

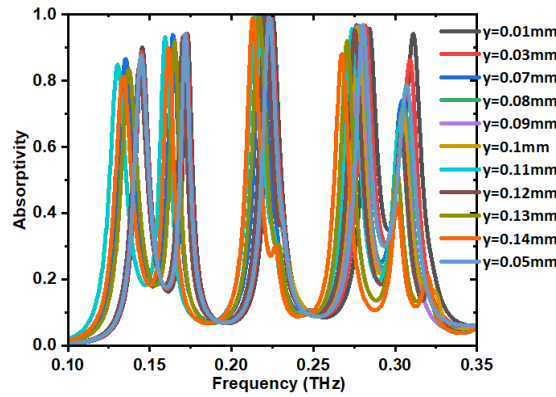


Fig. 6. Parametric study for quad and penta band operation in inner eclipse shaped patch structure (color online)

Table 3. No. of bands with respect to X and Y radius of inner small eclipse for quad and penta band

No. of bands	X and Y radius of inner small eclipse (mm)	Absorption rate (%)
4	0.12, 0.14	88,98.9,89.8,81
4	0.12, 0.13	91,99,91.6,81.8
4	0.12, 0.12	95.2,99.6,92.3,84.6
5	0.12, 0.10	70,96,99.7,92.8,85
4	0.12, 0.11	94.6,99.6,92,85
5	0.12, 0.09	70,95.8,99.6,92.7,85
5	0.12, 0.08	72,96.6,99.7,93.7,86
5	0.12, 0.05	78.6,96.8,99.7,93.9,87.5
5	0.12, 0.07	74,92,99.3,91.6,83.2
5	0.12, 0.03	86.2,97,99.8,94,88.6
5	0.12, 0.01	94,95,5,99.7,94,90

3.3. Parametric Study for Hexa band operation

Parameter study is used to choose the MMA with best absorption rate and maximum number of bands. From parametric analysis we found square patch resonator with etched eclipse structure [Fig. 2 (c)] based MMA gives the hexa number of bands. Etched eclipse structure having x radius and y radius. The ‘x’ radius is changed from 0.14

mm to 0.24 mm with the step size of 0.2 mm and the ‘y’ radius is changed from 0.26 mm to 0.45 mm which is shown in Fig. 7. When the radius of the x and y is 0.18 mm and 0.34 mm the simple planar MMA structure gives the hexa bands with the absorption rate of 92 %, 93 %, 99.9%, 88.5 %, 97 % and 82 % at the frequency of 0.146 THz, 0.174 THz, 0.227 THz, 0.288 THz, 0.315 THz and 0.328 THz respectively.

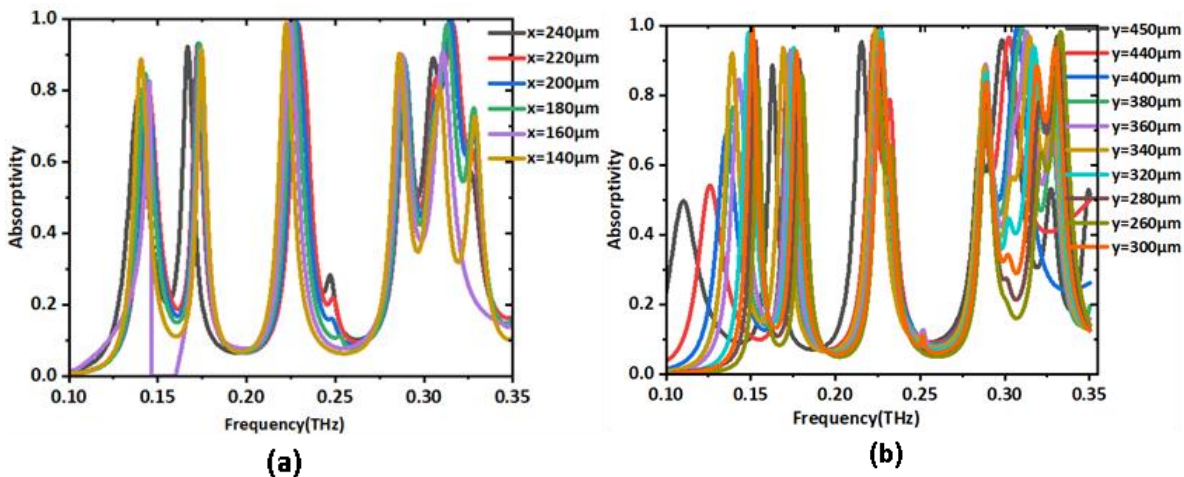


Fig. 7. Parametric study for hexa band operation in etched eclipse shaped patch structure (color online)

3.4. Polarization (ϕ) and angle stability (θ)

Polarization angle and oblique incident angle insensitive/sensitive nature of the structure is studied from changing the angle values from zero degree to ninety degree. In this part Polarization angle and oblique incident

angle insensitivity is checked for hexa band MMA. When we change the angle values from zero degree to ninety degree for both polarization and angle incidence condition, resonant frequency of the structure is not varied so this structure is Polarization angle and oblique incident angle insensitive in nature which is shown in Fig. 8.

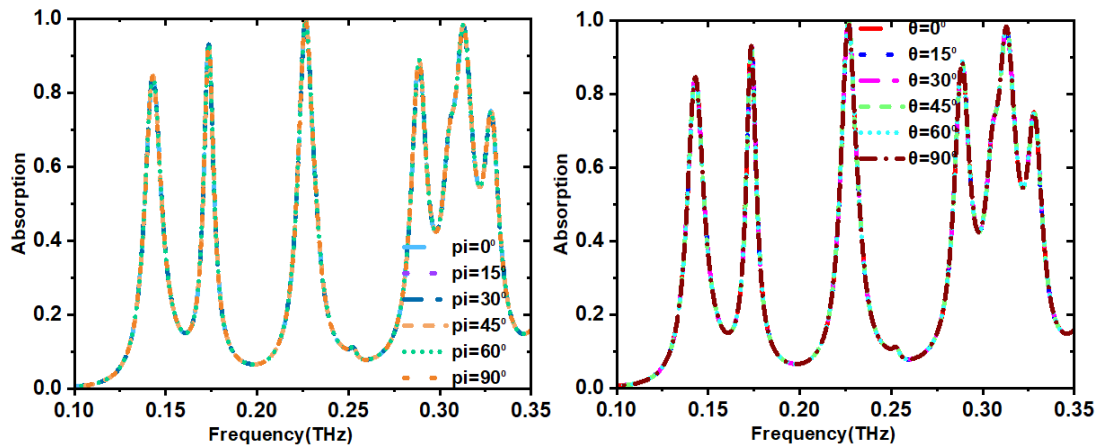


Fig. 8. Polarization (ϕ) and angle insensitivity (θ) of the MMA (color online)

3.5. Electric field distribution, magnetic field distribution and surface current distribution of Hexa band MMA

The physical mechanism of the structure is analysed from electric field distribution, magnetic field distribution and surface current distribution.

Electric field distribution for six band MMA is shown in Fig. 9. And the intensity scale is placed with electric current distribution plots. In all the six bands from (a) to (f), the intensity of the electric field distribution is maximum at surface of the dielectric and top patch

resonator fully. And the electric current distribution is good for all the six frequencies.

Magnetic field distribution for six band MMA is shown in Fig. 10. And the intensity scale is placed with magnetic current distribution plots. In all the six bands from (a) to (f), the intensity of the magnetic field distribution is maximum at surface of the dielectric and top patch resonator fully. Red and yellow colours mostly occupy the dielectric layer and top patch resonator so it indicates the maximum magnetic field distribution. And the magnetic current distribution is good for all the six frequencies.

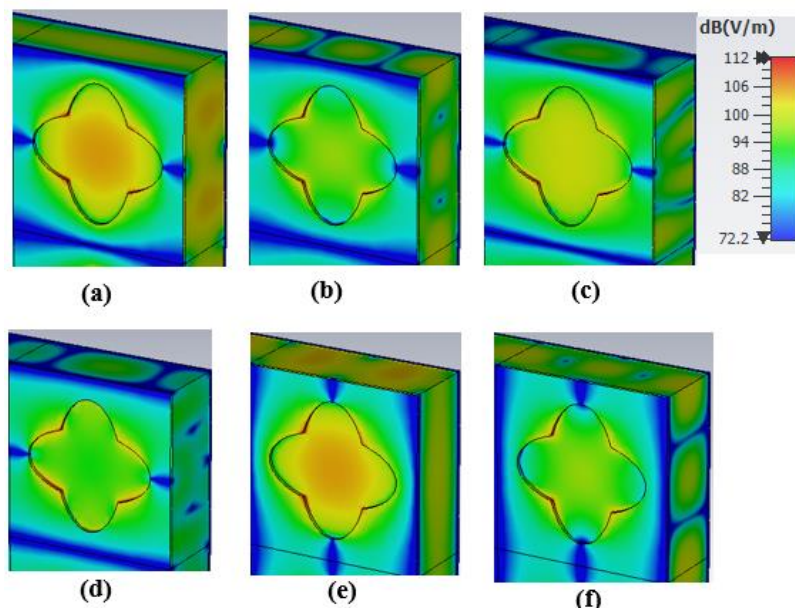


Fig. 9. Electric field distribution of MMA for six bands (a) 0.146 THz, (b) 0.174 THz, (c) 0.227 THz, (d) 0.288 THz, (e) 0.315 THz, (f) 0.328 THz (color online)

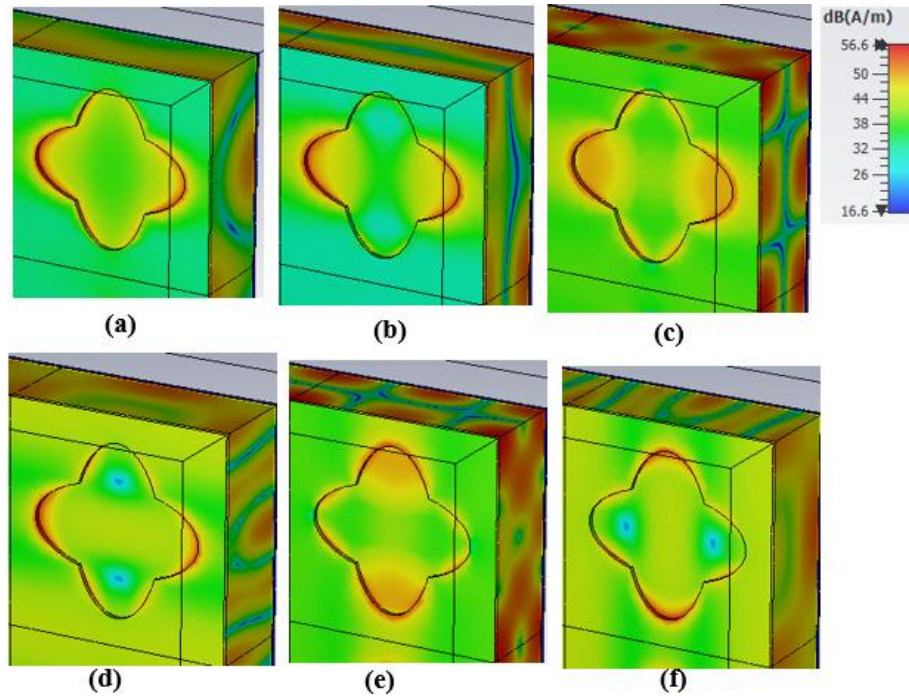


Fig. 10. Magnetic field distribution of MMA for six bands (a) 0.146 THz, (b) 0.174 THz, (c) 0.227 THz, (d) 0.288 THz, (e) 0.315 THz, (f) 0.328 THz (color online)

Table 4. Comparison of this work with previous bi/tri absorption functional works

Ref.	Unit cell thickness	Substrate thickness	Materials used	Working Frequency	No. of Layers	Absorption Functional	Polarization Stability	Angle Stability
[22]	(100×100) μm	5 μm	Au, Polyimide, Au, Si	0.5-1 THz	Multiple	Single-/Dual	insensitive	insensitive
[23]	(11×11) mm	0.25 mm	Cu, Teflon, Cu	6.64–17.38 GHz	Single	Single-/Penta	insensitive	insensitive
[24]	(60×60) μm	2 μm	Au, Polyimide, Au,	0.9-3.6 THz	Single	Dual/Triple	No analysis	No analysis
[25]	(60×60) μm	15 μm	Au, Si, Au	0-4.5 THz	Single	Single/Broad	No analysis	No analysis
[26]	(12.4×12.4) mm	0.035 mm	Cu, FR4, Cu	9.5–11 GHz	3 individual structures	Single/dual/triple	insensitive	No analysis
[27]	(12×12) mm	0.8 mm	Cu, FR4, Cu	8–12 GHz	3 individual structures	Single/dual/multi	insensitive	insensitive
[28]	(100×100) μm	19.8 μm	Au, Polyimide, Au,	0.5-2.5 THz	single	Quad band	No analysis	No analysis
[29]	(90×90) μm	40 μm	Au, Polyimide, Au,	0-2.4 THz	single	Penta band	No analysis	No analysis
[30]	(90×90) μm	8 μm	Au, InSb, Au	0.4-2 THz	single	Hexa band	insensitive	insensitive
This work	(0.45×0.45) mm		Copper, Polyimide	0.1-0.35 THz	Single	Quad-/Penta-/Hexa band	insensitive	insensitive

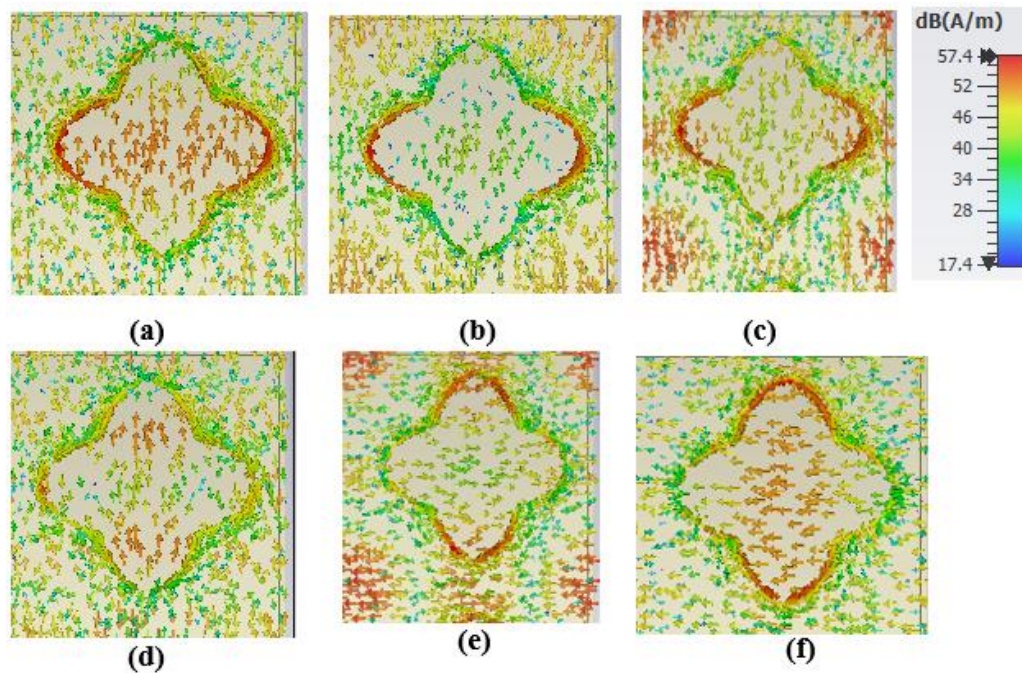


Fig. 10. Surface current distribution of MMA for six bands (a) 0.146 THz, (b) 0.174 THz, (c) 0.227 THz, (d) 0.288 THz, (e) 0.315 THz, (f) 0.328 THz (color online)

Surface current distribution for six band MMA is shown in figure 10. And the intensity scale is placed with Surface current distribution plots. In all the six bands from (a) to (f), the intensity of the Surface current distribution is maximum at surface of the dielectric and top patch resonator fully. Red and yellow colours mostly occupy the dielectric layer and top patch resonator in all directions so it indicates the maximum Surface current distribution. And the Surface current distribution is good for all the six frequencies.

4. Conclusion

The terahertz metamaterial absorbers for quad-/penta and hexa band operation is presented. Without using stacked layers or multiple Resonators in a single unit cell, the proposed absorber contains only three layers, polyimide substrate is placed in between the ground copper plane and top copper patch resonator. The top metallic structure consists of square shaped resonator. From that one horizontal and one vertical eclipse structure is etched and one horizontal and one vertical eclipse structure is added inside the etched eclipse structure. When we varying the inner eclipse x and y radius value, number of resonance bands and resonant frequency is also varied and this initial structure gives the quad band operation. It gives the Penta band operation when we change the inner eclipse y -radius value. Same structure gives the hexa band operation while deleting the total inner eclipse. These are all addressed in terms of the various stages of MMA design development. To create quad-/Penta and hexa bands in a single structure, parametric study is crucial. Electric field plots, magnetic field distribution plots, and surface current distribution

plots are used to analyse the physical structure. Curves of properties that are indifferent to polarisation and angle are explained. Applications for terahertz multiband and sensing will utilise the suggested structure.

References

- [1] C. M. Watts, X. Liu, W. J. Padilla, *Adv. Mater.* **24**, OP98 (2012).
- [2] M. K. Hedayati, F. Faupel, M. Elbahri, *Materials* **7**, 1221 (2014).
- [3] Y. Cai, Y. Guo, Y. Zhou, X. Huang, G. Yang, J. Zhu, *Opt. Express* **28**, 31524 (2020).
- [4] Y. Liu, R. Zhong, J. Huang, Y. Lv, C. Han, S. Liu, *Opt. Express* **27**, 7393 (2019).
- [5] B. X. Khuyen, B. S. Tung, Y. J. Yoo, Y. J. Kim, K. W. Kim, L. Y. Chen, V. D. Lam, Y. P. Lee, *Sci. Rep.* **7**, 45151 (2017).
- [6] Y. Cui, Y. He, Y. Jin, F. Ding, L. Yang, Y. Ye, S. Zhong, Y. Lin, S. He, *Laser Photonics Rev.* **8**, 495 (2014).
- [7] D. Wu, R. Li, Y. Liu, Z. Yu, L. Yu, L. Chen, C. Liu, R. Ma, H. Ye, *Nanoscale Res. Lett.* **12**, 427 (2017).
- [8] S. Ogawa, M. Kimata, *Materials* **11**, 458 (2018).
- [9] N. I. Landy, S. Sajuyigbe, J. J. Mock, D. R. Smith, W. J. Padilla, *Phys. Rev. Lett.* **100**, 207402 (2008).
- [10] X. Zhang, Z. Liu, *Nat. Mater.* **7**, 435 (2008).
- [11] S. Yoo, S. Lee, Q.-H. Park, *ACS Photonics* **5**(4), 1370 (2018).
- [12] D. Schurig, J. J. Mock, B. Justice, S. A. Cummer, J. B. Pendry, A. F. Starr, D. R. Smith, *Science* **314**(5801), 977 (2006).
- [13] F. Chuhuan, S. Fan, S. Jian, L. Qi, Y. Hongbin, *IEEE Photonics J.* **9**(4), 1 (2017).

- [14] Z. Shen, S. Li, Y. Xu, W. Yin, L. Zhang, X. Chen, *Phys. Rev. Appl.* **16**(1), 014066 (2021).
- [15] K. D. Xu, J. Li, A. Zhang, Q. Chen, *Opt. Express* **28**(8), 11482 (2020).
- [16] B. Zhang, K. Xu, *J. Opt. Soc. Am. B* **39**(3), A52 (2022).
- [17] T. Lv, G. Dong, C. Qin, J. Qu, B. Lv, W. Li, Z. Zhu, Y. Li, C. Guan, J. Shi, *Opt. Express* **29**(4), 5437 (2021).
- [18] S. Wan, C. Qin, K. Wang, Y. Li, C. Guan, B. Lv, W. Li, J. Shi, *J. Appl. Phys.* **131**(21), 213104 (2022).
- [19] Y. Lu, J. Li, S. Zhang, J. Sun, J. Q. Yao, *Appl. Opt.* **57**(21), 6269 (2018).
- [20] B. Mulla, C. Sabah C, *Physica E Low Dimens. Syst. Nanostruct.* **86**, 44 (2017).
- [21] C. Sabah, B. Mulla, H. Altan, L. Ozyuzer, *Pramana* **91**(2), 17 (2018).
- [22] S. Yuan, Rongcao Yang, Jianping Xu, Jiayun Wang, Jinping Tian, *Materials Research Express* **6**(7), 075807 (2019).
- [23] J. Wang, R. C. Yang, J. P. Xu, J. P. Tian, R. B. Ma, W. M. Zhang, *Materials* **11**, 16199 (2018).
- [24] B. X. Wang, C. Tang, Q. S. Niu, Y. B. He, T. Chen, *Nanoscale Research Letters* **14**(1), 64 (2019).
- [25] B. X. Wang, Y.-H. He, C. Tang, Q. S. Niu, F. W. Pi, *SN Applied Sciences* **2**(3), 393 (2020).
- [26] A. Bhati, K. R. Hiremath, *International Conference on Microwave and Photonics (ICMAP)*, Dhanbad, 1 (2015).
- [27] P. Jain, A. K. Singh, J. K. Pandey, S. Garg, S. Bansal, M. Agarwal, S. Kumar, N. Sardana, N. Gupta, A. K. Singh, *Microwaves, Antennas and Propagation* **14**, 390 (2020).
- [28] B.-X. Wang, G.-Z. Wang, *IEEE Photonics Journal* **8**(6), 1 (2016).
- [29] Ben-Xin Wang, Guiyuan Duan, Chongyang Xu, Jieying Jiang, Wei Xu, Fuwei Pi, *Materials and Design* **225**, 111586 (2023).
- [30] H. Zou, Y. Cheng, *Optical Materials* **88**, 674 (2019).

*Corresponding author: amitkr.varshney16@gmail.com